Journal of Fluids and Structures (1997) **11,** 597–615

INVESTIGATION OF IMPULSIVELY-STARTED FLOW AROUND SIDE-BY-SIDE CIRCULAR CYLINDERS: APPLICATION OF PARTICLE IMAGE VELOCIMETRY

D. Sumner, S. J. Price and M. P. Païdoussis
Department of Mechanical Engineering, McGill University, Montréal, Québec, Canada

(Received 13 December 1996 and in revised form 17 April 1997)

The impulsively-started flow field for two and three circular cylinders of equal diameter arranged side-by-side has been investigated using particle image velocimetry (PIV), over a transverse pitch ratio range of $T/D = 1{\cdot}0$–$3{\cdot}0$, and for Reynolds numbers from $\mathrm{Re} = 1500$ to 3000. The PIV technique was used to obtain a time history of the instantaneous in-plane vorticity field from the moment of impulsive start, from which the development of the flow was studied. Measurements of vortex strength and vortex position relative to the cylinders were obtained from these data. Two and three cylinder configurations of $T/D = 1{\cdot}0$ were found to exhibit a cursory degree of similarity to a single, isolated impulsively-started circular cylinder. Side-by-side configurations of $T/D > 1{\cdot}0$ were dominated by the strong gap flow(s) between the cylinders, the vortices generated alongside the gap flow(s), and the formation of a single counter-rotating vortex pair in the far-wake.

1. INTRODUCTION

The time evolution of the flow field for a single, isolated circular cylinder impulsively set into motion may be considered to be one of the classic examples of unsteady fluid dynamics. Its study has provided physical insight into a number of time-dependent fluid dynamic processes, including two-dimensional unsteady boundary layer formation and separation, and also vortex formation and vortex shedding. The flow field is primarily characterized by the formation of a symmetrical recirculation zone in the cylinder near-wake, containing a pair of stationary eddies of equal strength and opposite rotation. Eventually, these eddies are shed from the cylinder and the familiar steady flow pattern of periodic vortex shedding is initiated, provided the Reynolds number is sufficiently high. The impulsively-started flow field of the circular cylinder is also marked by the formation of small regions of secondary vorticity, located downstream of the point of boundary layer separation. These regions are not observed for a circular cylinder under steady cross-flow conditions.

Flow visualization and other experimental studies such as those of Honji & Taneda (1969), Nagata *et al.* (1975, 1979, 1985a, b, 1989), Coutanceau & Bouard (1977), Bouard & Coutanceau (1980), Wu & Chu (1989) and Chu & Liao (1992) provide a detailed quantitative description of the recirculation zone development for Reynolds numbers up to and greater than 10 000. Sarpkaya (1991) and others have investigated the behaviour of the unsteady lift and drag forces. The flow field has also been investigated numerically, with some success for low Reynolds numbers and small elapsed times, by Ta Phuoc Loc & Bouard (1985) and others.

Small groups of circular cylinders in close proximity, however, have not been investigated as extensively under unsteady conditions. Recent flow visualization

0889–9746/97/060597 + 19 $25.00/fl970097

experiments (Sumner *et al*. 1997a) have outlined, for the first time, the complex starting flow dynamics for two and three circular cylinders arranged in a side-by-side configuration, and the effects of varying the separation distance between them. In this study, further insight into the fluid behaviour is obtained through the application of particle image velocimetry (PIV), to provide a detailed quantitative description of the vortex dynamics.

2. DESCRIPTION OF THE FLOW FIELD

The flow field of a single circular cylinder of diameter D impulsively set into motion at cross-flow velocity U, as shown in Figure 1(a), is marked by the temporal development of a recirculation zone of length L_R measured from the base of the cylinder, in the streamwise direction x. The recirculation zone contains a pair of primary eddies located at streamwise position a measured from the base of the cylinder, and separated by a distance b in the cross-stream or transverse direction y. The strength of a primary eddy may be expressed as the circulation magnitude Γ computed along the path of integration shown in Figure 1(b). In the context of the in-plane vorticity field denoted by ω_z, the length L_R may be defined as the downstream extent of appreciable measured vorticity, a criterion that is independent of the motion reference frame;

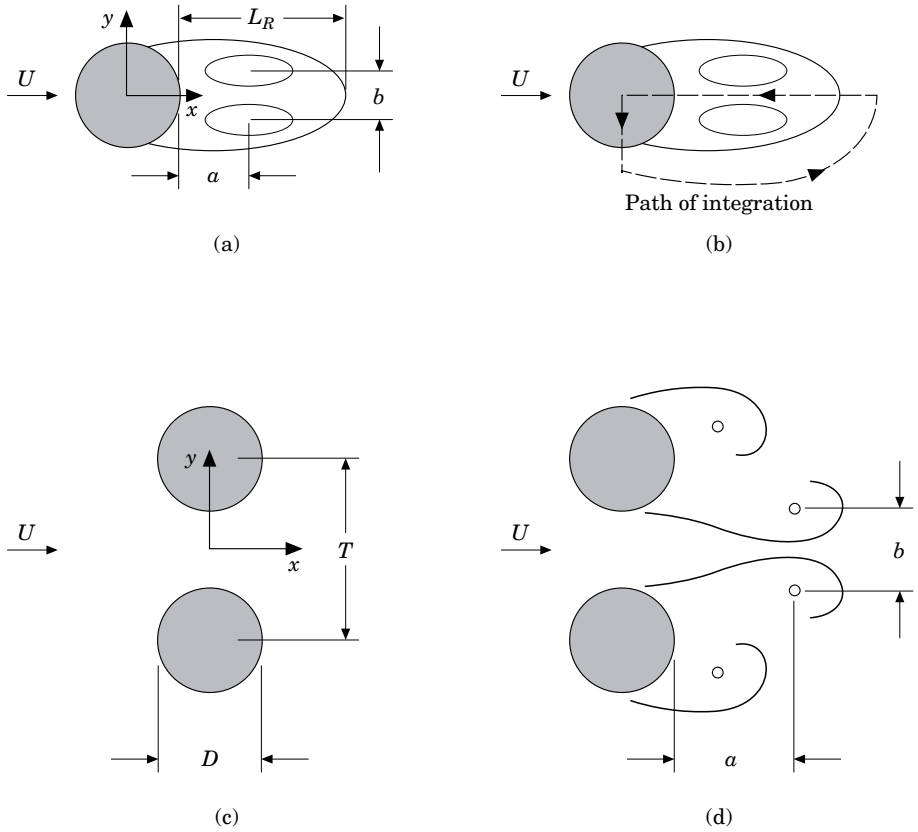

Figure 1. Nomenclature for impulsively-started circular cylinders of equal diameter D: (a) single, isolated circular cylinder, showing the parameters for the recirculation zone and the primary eddies; (b) the path of integration used to compute the circulation of a primary eddy; (c) two circular cylinders arranged side-by-side; (d) vortex centre position nomenclature for side-by-side circular cylinders with $T/D > 1{\cdot}0$.

otherwise, L_R may be defined in a nominally equivalent manner as the streamwise location where the local fluid velocity becomes sensibly equal to the constant cross-flow velocity U.

Configurations of two and three circular cylinders of equal diameter D arranged side-by-side are denoted by the centre-to-center transverse pitch ratio T/D separating the cylinders, as shown in Figure 1(c). Similar definitions of a and b may be used for the streamwise and cross-stream positions of vortex centres, as shown in Figure 1(d).

3. EXPERIMENTAL APPROACH

In this study, the temporal development of the flow field for a single, isolated impulsively-started circular cylinder, and for configurations of two and three circular cylinders arranged side-by-side, were investigated through the use of particle image velocimetry (PIV) (Willert & Gharib 1991). This work represents one of the first known applications of the PIV technique to unsteady bluff-body flows. For each configuration of cylinders, the technique was used to obtain the time history of the nondimensional instantaneous in-plane vorticity field, $\omega_z D/U$, as the flow developed over a range of nondimensional elapsed time t^* $(=tU/D)$; the measurement uncertainty in t^* was estimated at 5%. Experiments were conducted in a small vertical water towing tank of dimensions 305 mm × 610 mm × 1200 mm, as illustrated in Figure 2. Plexiglas cylinder models of $D = 25{\cdot}4$ mm were mounted in a cantilevered fashion from a flat plate, and were pulled upwards through stationary fluid at velocities of $U = 60$ mm/s–110 mm/s after a nearly-impulsive start, yielding Reynolds numbers of Re = 1500–3000. The gap between the free ends of the cylinders and the tank wall remained less than $0{\cdot}2D$. Each cylinder had an aspect ratio of 9·0, and a solid blockage ratio of 4·2%. For most of the tests, the nondimensional acceleration parameter A_p $(=DU^{-2}(\mathrm{d}u/\mathrm{d}t)$, for streamwise acceleration $\mathrm{d}u/\mathrm{d}t$, and actual cylinder velocity

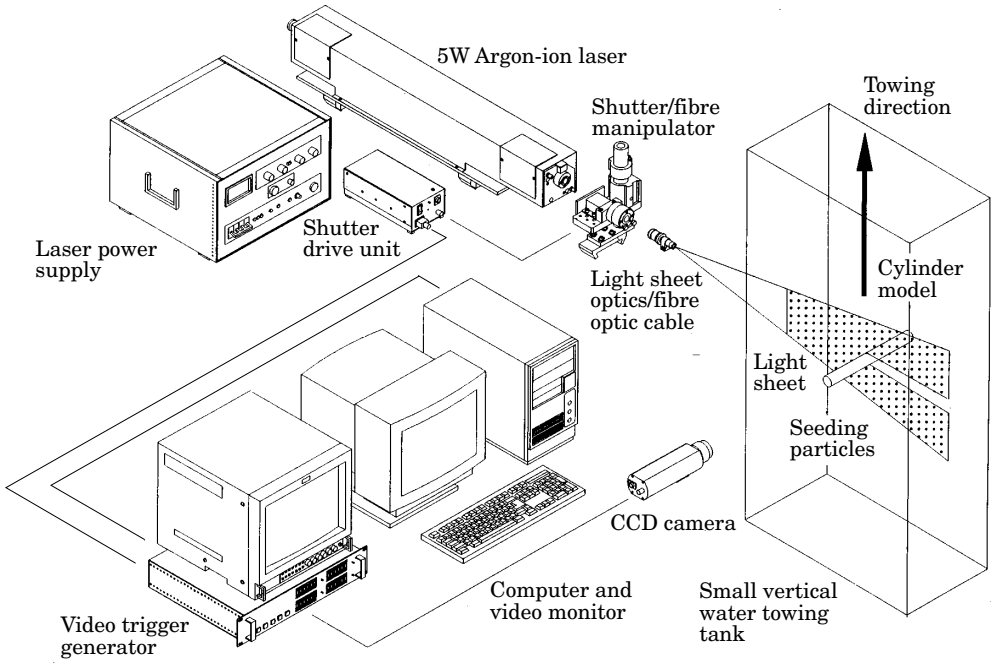

Figure 2. Schematic of the experimental apparatus and digital PIV instrumentation.

$u \leq U$) ranged from 0·3 to 0·7, indicating that nearly-impulsively-started conditions were usually achieved (Sarpkaya 1991). Results were rejected from a small number of tests for which $A_p < 0{\cdot}3$, since this meant the cylinders were more slowly accelerated to a constant velocity U, rather than impulsively-started. The velocity of the cylinders was determined from the digital particle images and the PIV data, as discussed below, with an estimated measurement uncertainty of 3%.

For the application of PIV, the water was seeded with irregularly-shaped, nearly neutrally-buoyant latex particles, approximately 500 μm in effective diameter. A section of the flow was illuminated with a pulsed light sheet generated by a 5 W argon-ion laser passing through a mechanical shutter, and successive pairs of single-exposed digital particle images (each of 512×480 pixels) were acquired with a Dantec Double Image 700 CCD camera and frame grabber. The image exposure time was typically 5 ms, the time between single-exposed images comprising a pair was typically 6 ms, and the time between successive pairs (or sets of vorticity data) was 0·2 s. Dantec FlowGrabber digital PIV software employing a cross-correlation algorithm was used to compute the raw displacement vector field from the particle image data, using an interrogation window of 32×32 pixels with 75% overlap. Software developed in-house was used to compute the velocity and vorticity fields in the presence of the cylinder models, which typically covered a field of approximately 150 mm $\times$ 150 mm.

4. SINGLE CIRCULAR CYLINDER

The impulsively-started flow about a single circular cylinder was examined first. The development of the instantaneous in-plane velocity and vorticity fields for $\mathrm{Re} = 1500$ are shown in Figure 3. In Figure 3(a) the velocity field is shown in the experiment reference frame, with the cylinder being towed and the fluid initially stationary; in Figure 3(b), the local cylinder velocity $u \leq U$ has been superimposed on the velocity field, to create an inertial reference frame; in both cases, the velocity vector data have been rendered nondimensional using the towing velocity U. The vorticity contour data shown in Figure 3(c), expressed in nondimensional form as $\omega_z D/U$, may be computed from either velocity field since it is independent of the reference frame (unlike the more popular streamline representation). In this and subsequent figures, the smallest magnitude vorticity contour plotted was typically chosen to be 10% of the maximum vorticity in the flow field. The measurement uncertainty of the vorticity data from PIV has been estimated at 10%.

The nondimensional geometrical parameters a/D, b/D, and L_R/D, governing the structure of the recirculation zone, as well as the nondimensional primary eddy circulation Γ/UD, were determined from a number of experiments covering $\mathrm{Re} =$ 1500–1900. The positions of the primary eddies, defined by a/D and b/D, were determined graphically from the vorticity contour data, and correspond to the geometric centres of the regions of appreciable vorticity defining the eddies, rather than the locations of maximum vorticity magnitude. The length of the recirculation zone, L_R/D, was found by determining the downstream extent of the contours of minimum vorticity magnitude that sensibly defined the zone in question. The measurement uncertainty associated with the nondimensional geometrical parameters a/D, b/D, and L_R/D was estimated at no more than 5%. For the nondimensional primary eddy circulation Γ/UD, the closed path of integration corresponded to the contour line of minimum vorticity magnitude sensibly enclosing the eddy, bounded on

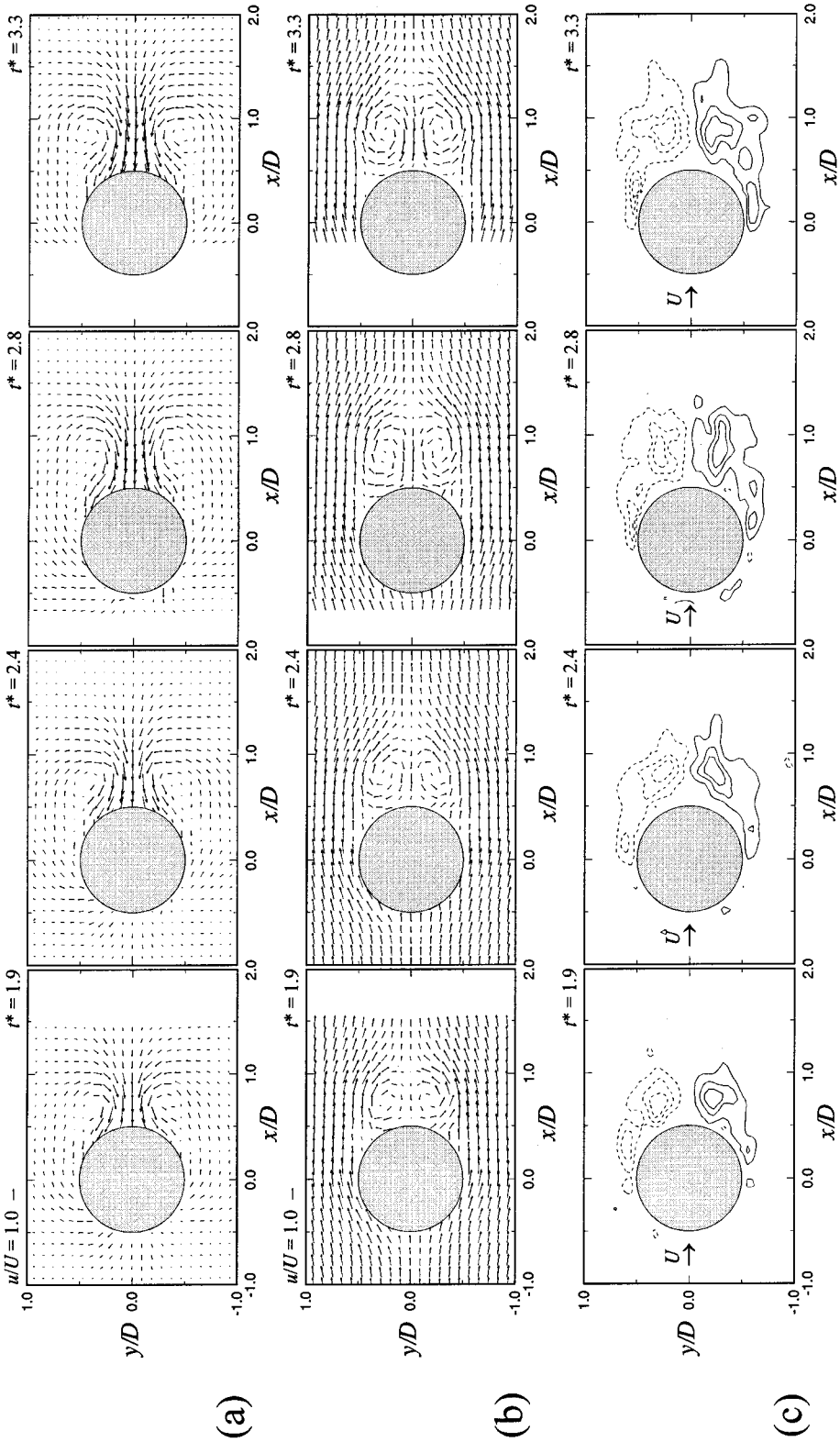

Figure 3. Single circular cylinder impulsively set into motion, Re = 1500, A_p = 0·5: (a) nondimensional instantaneous in-plane velocity field, representing the experiment reference frame, with the cylinder towed from right to left through stationary fluid; every second vector omitted for clarity; (b) nondimensional instantaneous in-plane velocity field, with instantaneous towing velocity superimposed to obtain an inertial reference frame; every second vector omitted for clarity; (c) nondimensional instantaneous in-plane vorticity field, with a minimum vorticity contour magnitude of 2·0 and a contour interval of 4·0; dashed lines represent negative (CW) vorticity.

the upstream side by the y-axis at the centre of the cylinder. The measurement uncertainty associated with Γ/UD was estimated to be 10%.

The data for a/D, b/D, L_R/D, and Γ/UD were found to compare favourably with previously published data, as shown in Figure 4. Small differences between the published eddy circulation data (Nagata *et al.* 1989) and those obtained from the PIV data, as shown in Figure 4(d), reflect the extreme sensitivity and difficulty of computing such quantities (Nagata *et al.* 1985b). Apart from providing some of the first full-field, instantaneous vorticity data for an impulsively-started circular cylinder, the results indicated that the experimental apparatus could reliably generate impulsively-started motion.

5. SIDE-BY-SIDE CONFIGURATIONS WITH $T/D = 1{\cdot}0$

The case of two or three circular cylinders of equal diameter arranged side-by-side is examined next, first with $T/D = 1{\cdot}0$, i.e. with the cylinders in contact with one another. In this case, the temporal development of the flow field exhibits similarity to that of a single cylinder.

The vorticity data shown in Figure 5 illustrate the gradual formation of a large recirculation zone containing a pair of symmetric eddies of opposite rotation, similar to that observed in previous flow visualization experiments (Sumner *et al.*, 1997a). Similarity between the single cylinder and side-by-side configurations with $T/D = 1{\cdot}0$ extends to the behaviour of geometrical parameters L_R/D and a/D, as well as the nondimensional primary eddy circulation Γ/UD, shown in Figure 6. In this figure, the data for two and three cylinders, and the elapsed time, are made nondimensional with the single cylinder diameter D, rather than using $2D$ or $3D$ as the case may be; use of the latter geometrical scales to render the data dimensionless did not yield a collapse of the data, even for b/D. That the recirculation zone parameters for single and multiple side-by-side circular cylinders do not collapse onto common curves reflects the obvious differences in the shape of the base region between two or three side-by-side cylinders and a single cylinder of two or three times the diameter. Data for L_R/D were also compared to similar measurements for a flat plate (Taneda & Honji 1971), but no apparent convergence of the multiple cylinder data with the flat plate data is observed for three adjacent cylinders.

6. SIDE-BY-SIDE CONFIGURATIONS WITH $T/D > 1{\cdot}0$

Two and three circular cylinders in a side-by-side configuration were then tested under impulsively-started conditions for $T/D > 1{\cdot}0$ and up $T/D = 3{\cdot}0$ for the two-cylinder system. For each of the configurations, the temporal evolution of the vorticity field was determined, and was found to be consistent with the fluid behaviour observed in previous flow visualization experiments (Sumner *et al.* 1997a). The flow fields remain symmetrical for each pitch ratio T/D examined and at each step in the time history: no evidence of an asymmetrical or biased flow pattern is observed, as is commonly noted under steady flow conditions (Bearman & Wadcock 1973; Eastop & Turner 1982; Kumada *et al.* 1984; Williamson 1985; Sumner *et al.* 1997b).

6.1. Two Side-by-Side Circular Cylinders with $T/D > 1{\cdot}0$

Vorticity data corresponding to the two-cylinder configurations are shown in Figure 7. From $T/D = 1{\cdot}5$ to $T/D = 3{\cdot}0$, symmetric and stable recirculation zones are not observed in the near-wake regions of the individual cylinders. Rather, the structure of

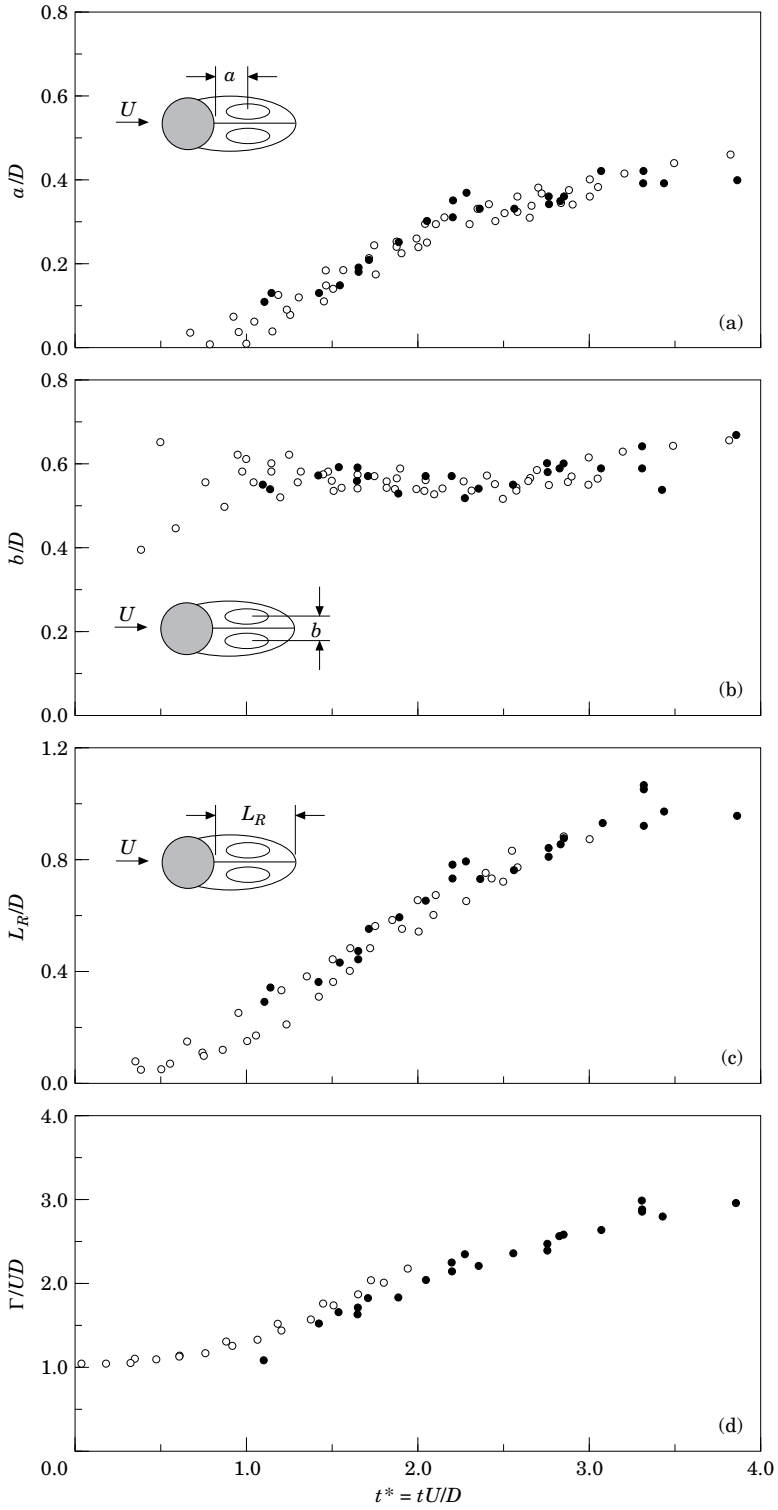

Figure 4. Recirculation zone data for a single, isolated, impulsively-started circular cylinder: (a) streamwise position of the primary eddies from the base of the cylinder; (b) cross-stream or transverse separation of the primary eddies; (c) streamwise extent of the recirculation zone from the base of the cylinder; (d) circulation or strength of a primary eddy. (○) Published data for Re = 1000–3000 (Bouard & Coutanceau 1980; Nagata *et al*. 1989; Wu & Chu 1989; Chu & Liao 1992); (●) present PIV experiments.

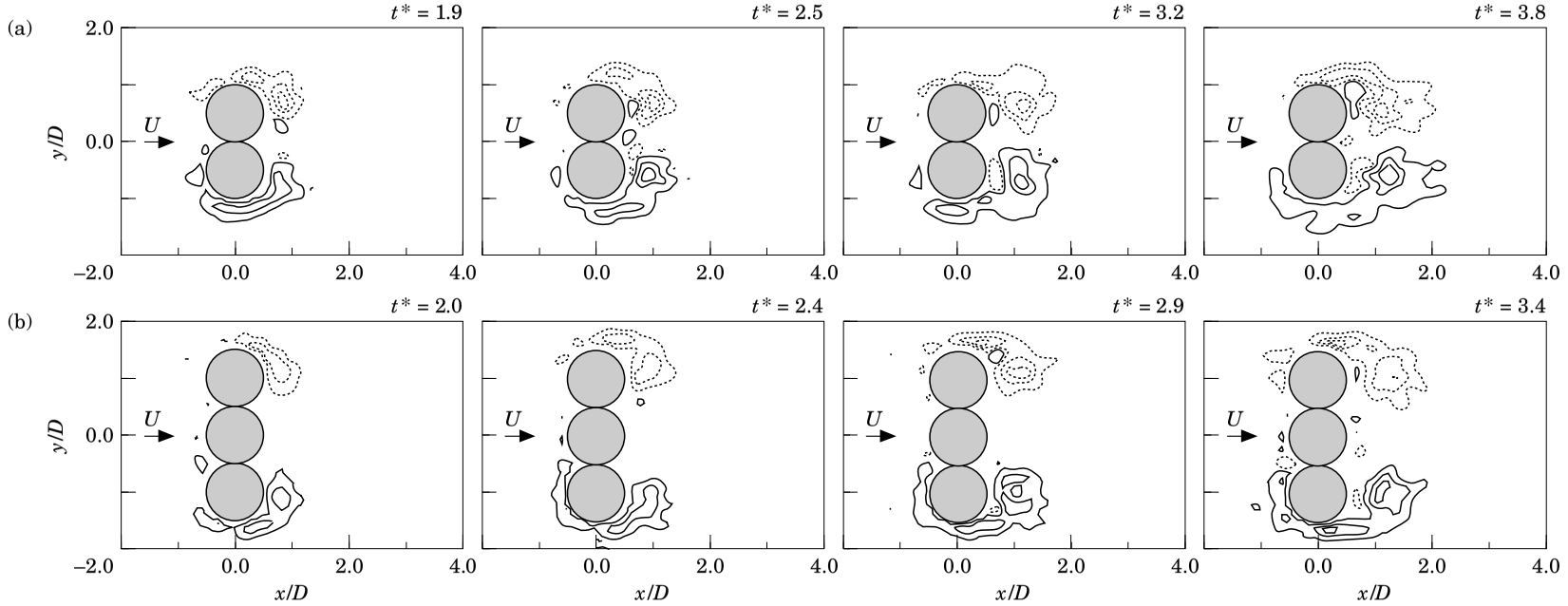

Figure 5. Development of the nondimensional instantaneous in-plane vorticity field for two and three side-by-side circular cylinders with $T/D = 1{\cdot}0$ impulsively set into motion: (a) two cylinders, Re = 2000, $A_p = 0{\cdot}3$; (b) three cylinders, Re = 1600, $A_p = 0{\cdot}3$. Minimum vorticity contour magnitude of 1·0, and contour interval of 4·0. Dashed lines represent negative (CW) vorticity.

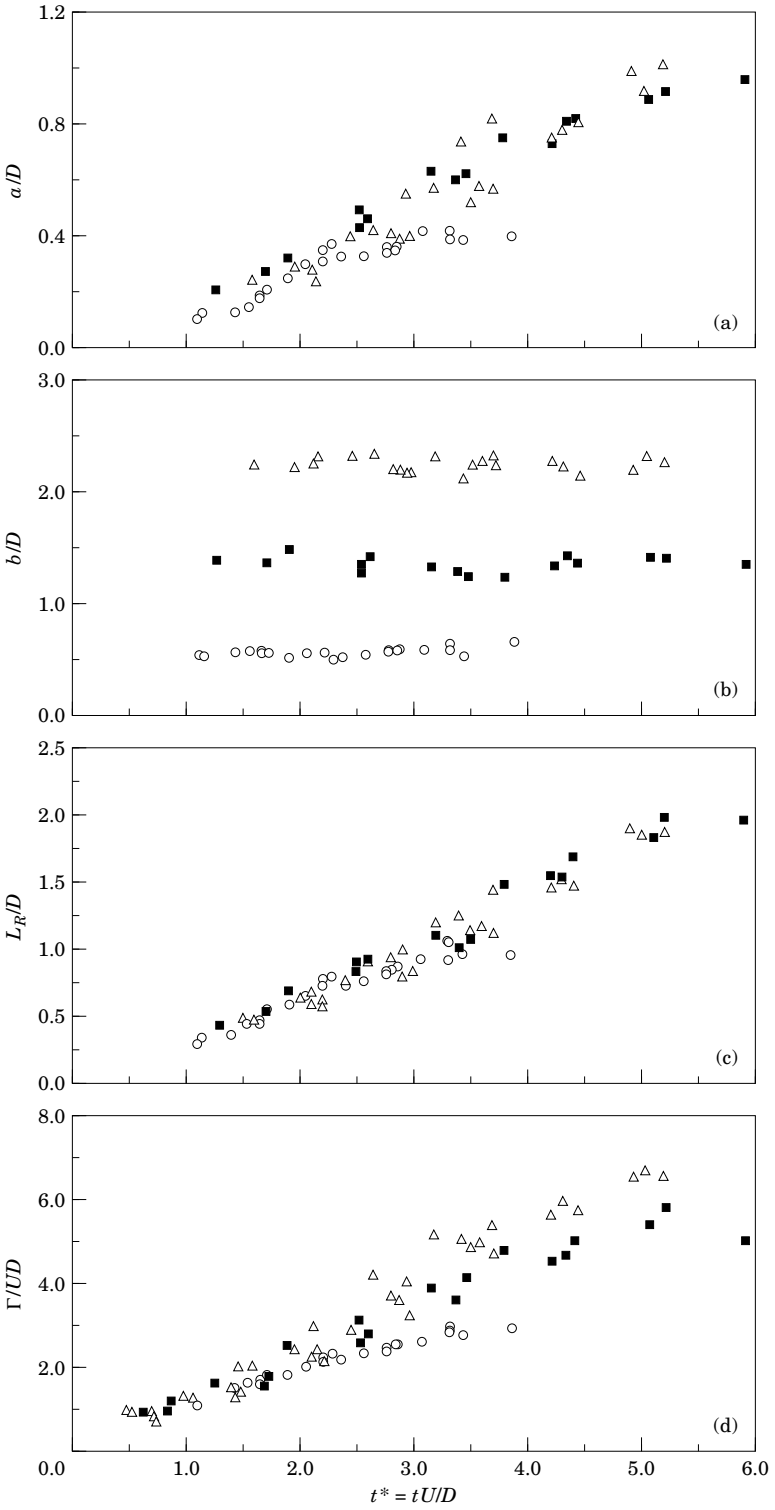

Figure 6. Recirculation zone data for a single, isolated, impulsively-started circular cylinder, and for side-by-side configurations of two and three circular cylinders with $T/D = 1{\cdot}0$; (○) one cylinder data; (■) two cylinder data; (△) three cylinder data: (a) streamwise position of the primary eddies from the base of the cylinder(s); (b) cross-stream or transverse separation of the primary eddies; (c) streamwise extent of the recirculation zone from the base of the cylinder(s); (d) circulation or strength of a primary eddy.

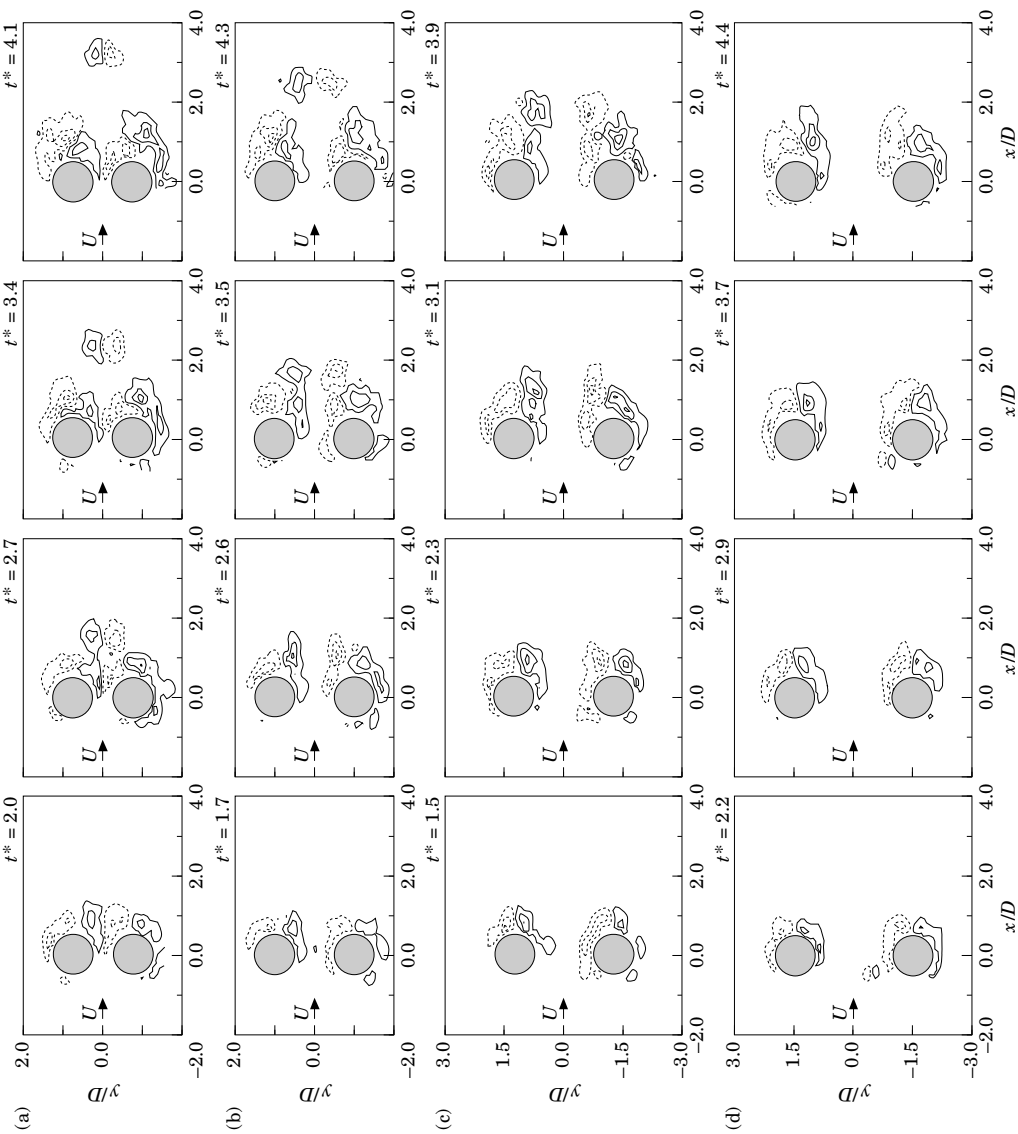

Figure 7. Development of the nondimensional instantaneous in-plane vorticity field for two side-by-side circular cylinders with $T/D > 1{\cdot}0$ impulsively set into motion: (a) $T/D = 1{\cdot}5$, Re = 2200, $A_p = 0{\cdot}3$; (b) $T/D = 2{\cdot}0$, Re = 2800, $A_p = 0{\cdot}3$; (c) $T/D = 2{\cdot}5$, Re = 2500, $A_p = 0{\cdot}7$; (*d*) $T/D = 3{\cdot}0$, Re = 2300, $A_p = 0{\cdot}3$. Minimum vorticity contour magnitude of 1·5, and contour interval of 4·0. Dashed lines represent negative (CW) vorticity.

the wake region is dominated by a strong gap flow between the cylinders, and rapid formation, shedding, and interaction of vortices alongside the gap flow. The gap flow initiates the breakup of the recirculation zones and vortex shedding much sooner in the time evolution than for a single cylinder. The far wake region is marked by the formation of a single counter-rotating vortex pair (that is usually symmetrical in both alignment with the flow axis and in the strengths of the two vortices) for $T/D = 1{\cdot}5$–$2{\cdot}5$. Shedding of the initial gap vortices is estimated to occur at $t^* = 2{\cdot}5$–$3{\cdot}0$, $t^* = 3{\cdot}0$–$3{\cdot}5$, and $t^* = 3{\cdot}5$–$4{\cdot}0$ for pitch ratios of $T/D = 1{\cdot}5$, $2{\cdot}0$ and $2{\cdot}5$, respectively. Shedding of the initial gap vortices is not observed, however, at a pitch ratio of $T/D = 3{\cdot}0$ (at least up to $t^* = 5{\cdot}5$), and consequently no counter-rotating vortex pair forms. For those pitch ratios where shedding is observed, new gap vortices form once the initial gap vortices are shed, and the near-wake region once again contains a pair of asymmetrical, quasi-attached recirculation zones.

The strength of the initially-formed vortices is shown in Figure 8 for each of the pitch ratios, revealing in most instances a steady increase in vortex strength with time and a reduction in vortex strength once a vortex is shed. The gap vortices (denoted by A) and the outer vortices (denoted by B) are approximately of equal magnitude of circulation and, along with the strengths of vortices that are still attached to the cylinders, are basically independent of T/D. The spread of the circulation data may be attributed to small differences in A_p from one T/D configuration to another, and particularly at $T/D = 2{\cdot}5$ and $3{\cdot}0$; as mentioned, A_p was found to vary from $0{\cdot}3$ to $0{\cdot}7$, with the majority of results obtained with $A_p = 0{\cdot}3$.

The streamwise location a and cross-stream separation b of like vortices, defined in Figure 1(d), are presented in Figure 9 for each T/D. Data for a/D reveal rapid streamwise acceleration of the initial gap vortices (A-vortices) for $T/D = 1{\cdot}5$–$2{\cdot}5$, and similar but less accentuated behaviour for the outer vortices (B-vortices). The acceleration of the gap vortices varies markedly with T/D, whereas the streamwise location of the outer vortices is generally independent of T/D. Cross-stream separation data b/D show the movement of the initially-shed gap vortices towards the flow axis, and some movement of the outer vortices.

A close examination of the flow patterns, circulation data, and vortex position data shown in Figures 7, 8, and 9 seems to suggest a different sort of fluid behaviour at $T/D = 3{\cdot}0$ compared with $T/D \leq 2{\cdot}5$. Such a distinction for $T/D > 2{\cdot}5$ is not entirely unexpected, since under steady conditions $T/D = 2{\cdot}2$–$2{\cdot}5$ represents the upper limit of critical pitch ratio and significant proximity interference, beyond which biased flow conditions are no longer observed (Bearman & Wadcock 1973; Williamson 1985; Sumner *et al*. 1997b). An examination of the temporal and streamwise development of the nondimensional instantaneous gap flow velocity profile at each T/D did not provide any additional insight into this apparent change in behaviour.

6.2. Three Side-by-Side Circular Cylinders with $T/D > 1{\cdot}0$

The time evolution of the vorticity field for the three-cylinder configurations of $T/D = 1{\cdot}5$ and $2{\cdot}0$ is shown in Figure 10. For both pitch ratios, the flow field is symmetric about the central cylinder, with biased near-wake regions for the outer cylinders. Highly complex vortex interactions occur. At $T/D = 1{\cdot}5$ in Figure 10(a), shedding of the gap vortices from the outer cylinders inhibits the immediate formation of a recirculation zone behind the central cylinder. These gap vortices interact strongly with one another across the combined wake of the three cylinders. The outer gap vortices also dominate the early development of the flow for $T/D = 2{\cdot}0$, seen in Figure 10(b).

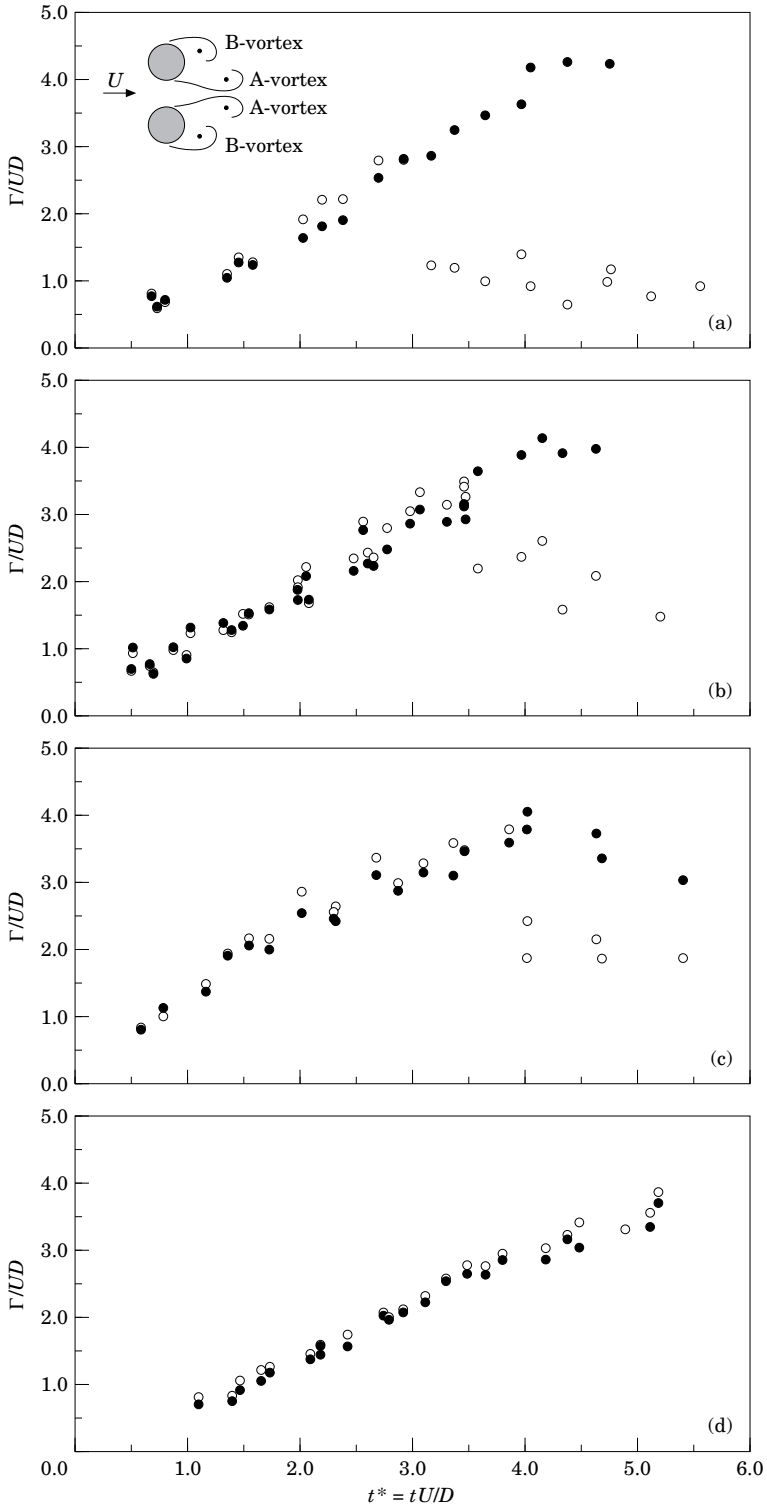

Figure 8. Vortex strength data for two side-by-side circular cylinders with $T/D > 1{\cdot}0$ impulsively set into motion; (○) A-vortices; (●) B-vortices: (a) $T/D = 1{\cdot}5$; (b) $T/D = 2{\cdot}0$; (c) $T/D = 2{\cdot}5$; (d) $T/D = 3{\cdot}0$.

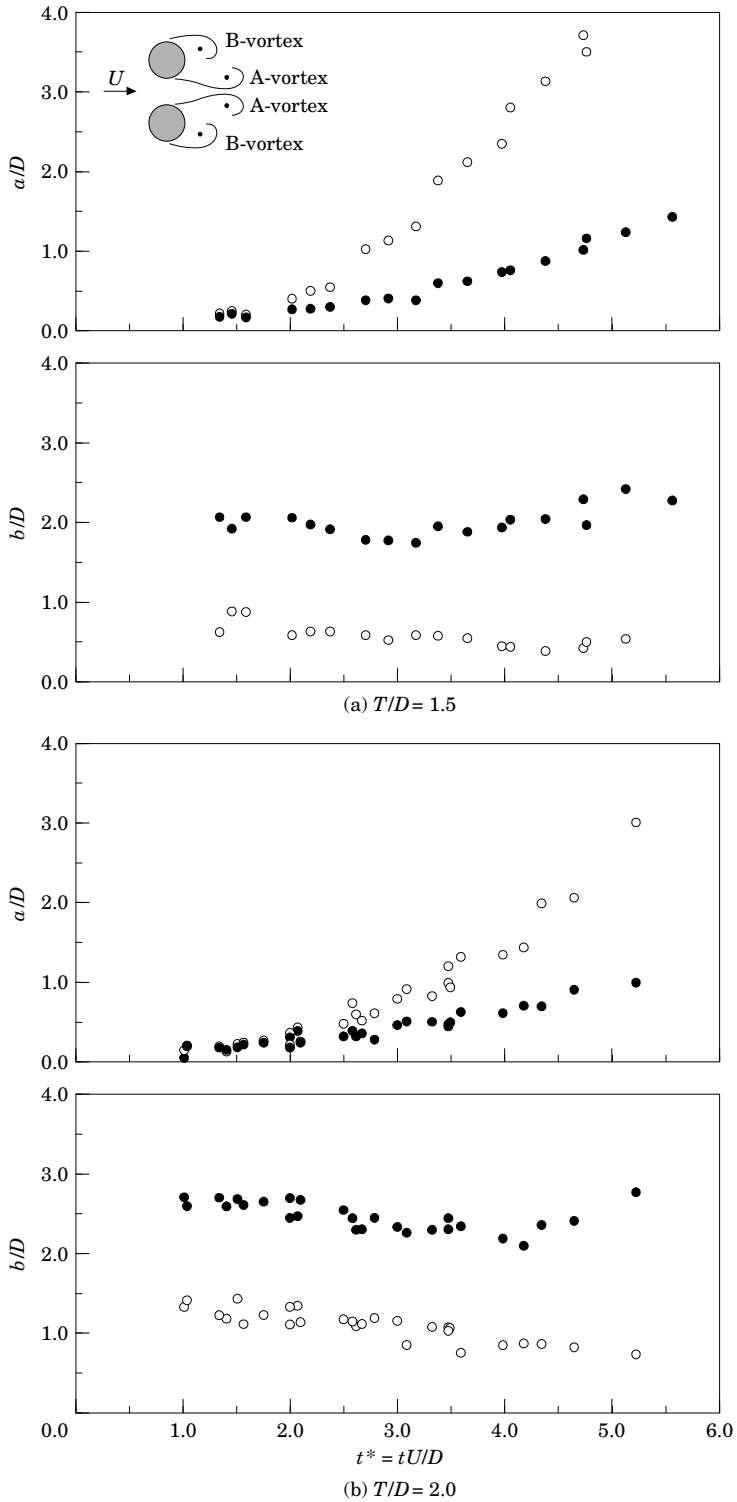

Figure 9. Vortex centre position data a/D and b/D for two side-by-side circular cylinders with $T/D > 1{\cdot}0$ impulsively set into motion; (○) A-vortices; (●) B-vortices: (a) $T/D = 1{\cdot}5$; (b) $T/D = 2{\cdot}0$; (c) $T/D = 2{\cdot}5$; (d) $T/D = 3{\cdot}0$.

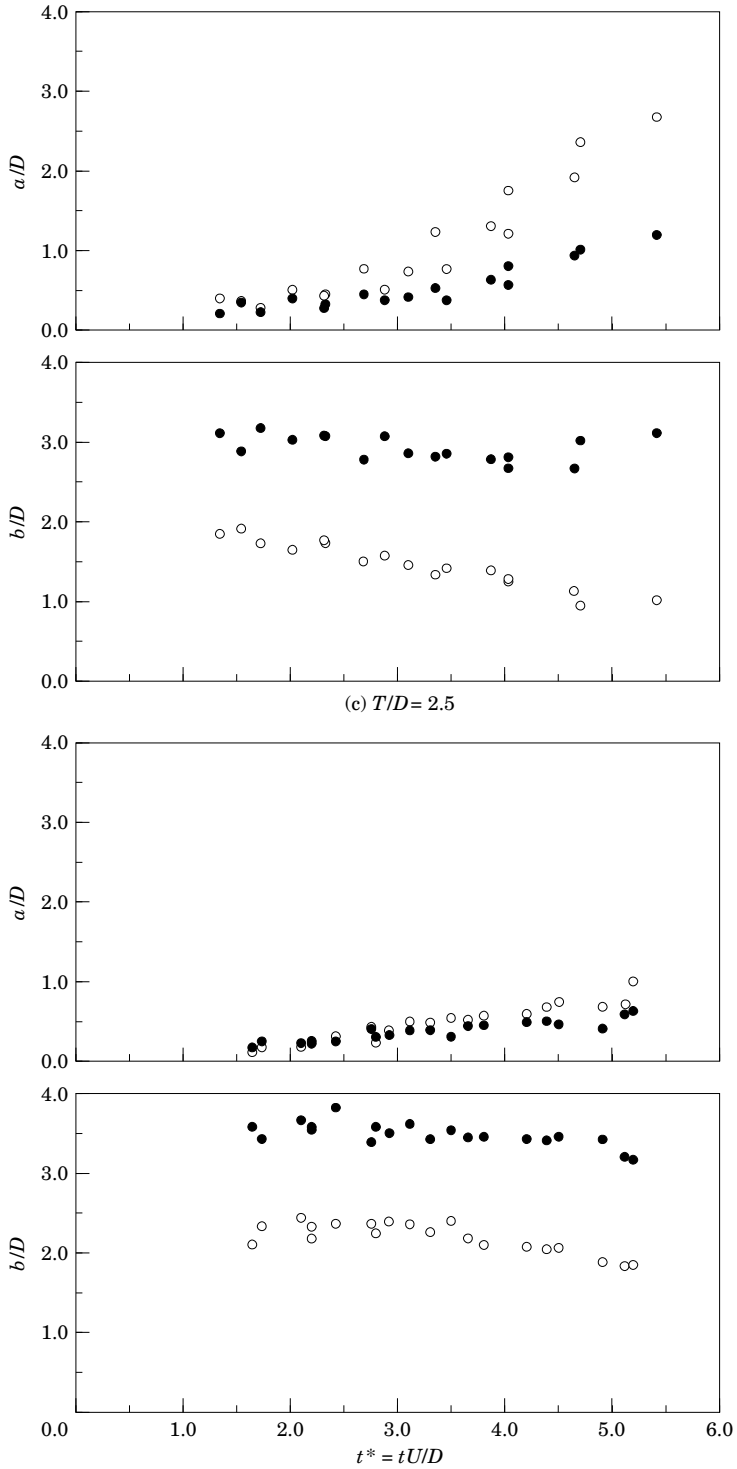

(c) $T/D = 2.5$

(d) $T/D = 3.0$

Figure 9. (*Continued*.)

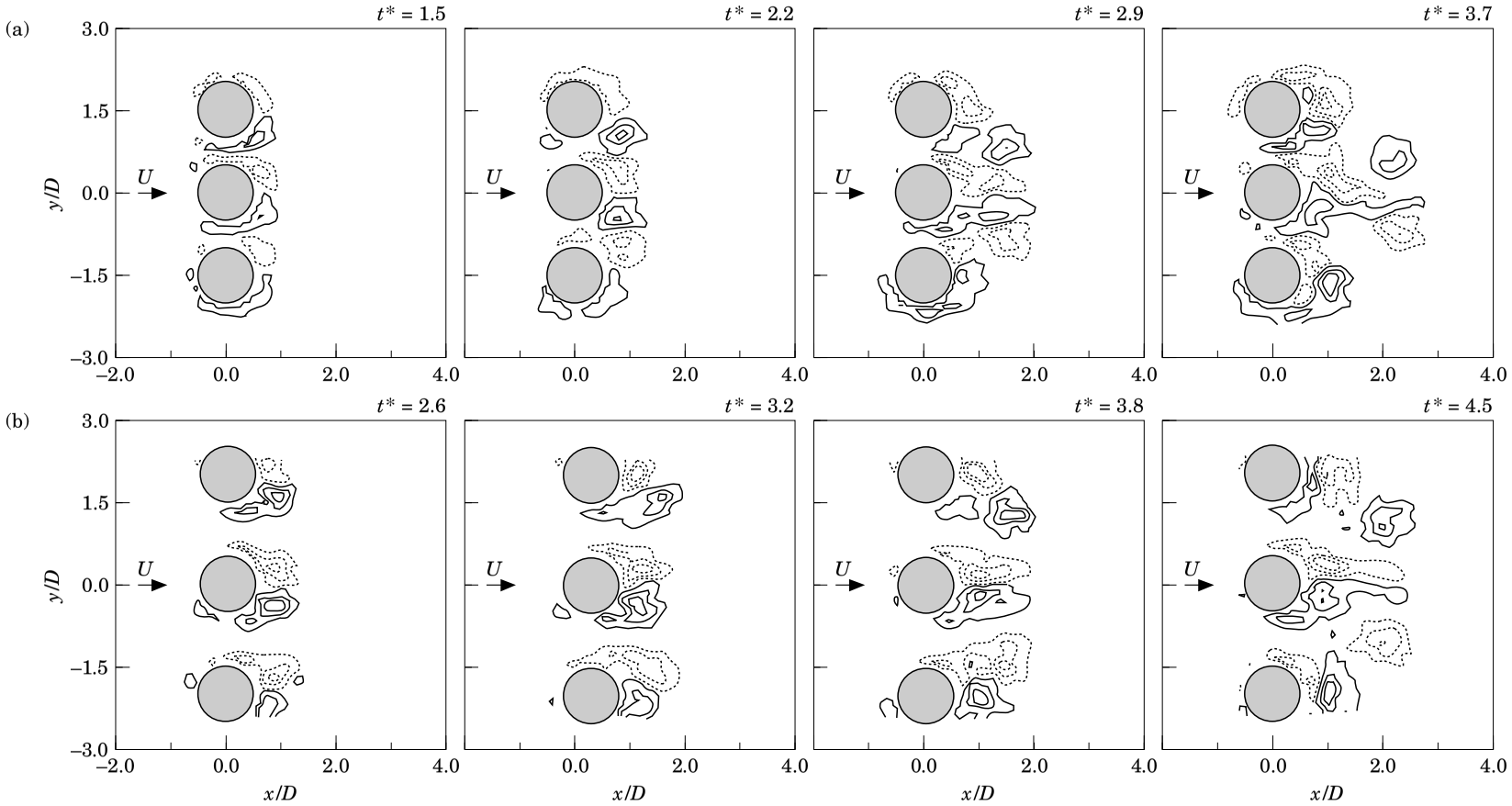

Figure 10. Development of the nondimensional instantaneous in-plane vorticity field for three side-by-side circular cylinders with $T/D > 1{\cdot}0$ impulsively set into motion: (a) $T/D = 1{\cdot}5$, Re = 2300, $A_p = 0{\cdot}3$; (b) $T/D = 2{\cdot}0$, Re = 2000, $A_p = 0{\cdot}4$. Minimum vorticity contour magnitude of 1·5, and contour interval of 4·0. Dashed lines represent negative (CW) vorticity.

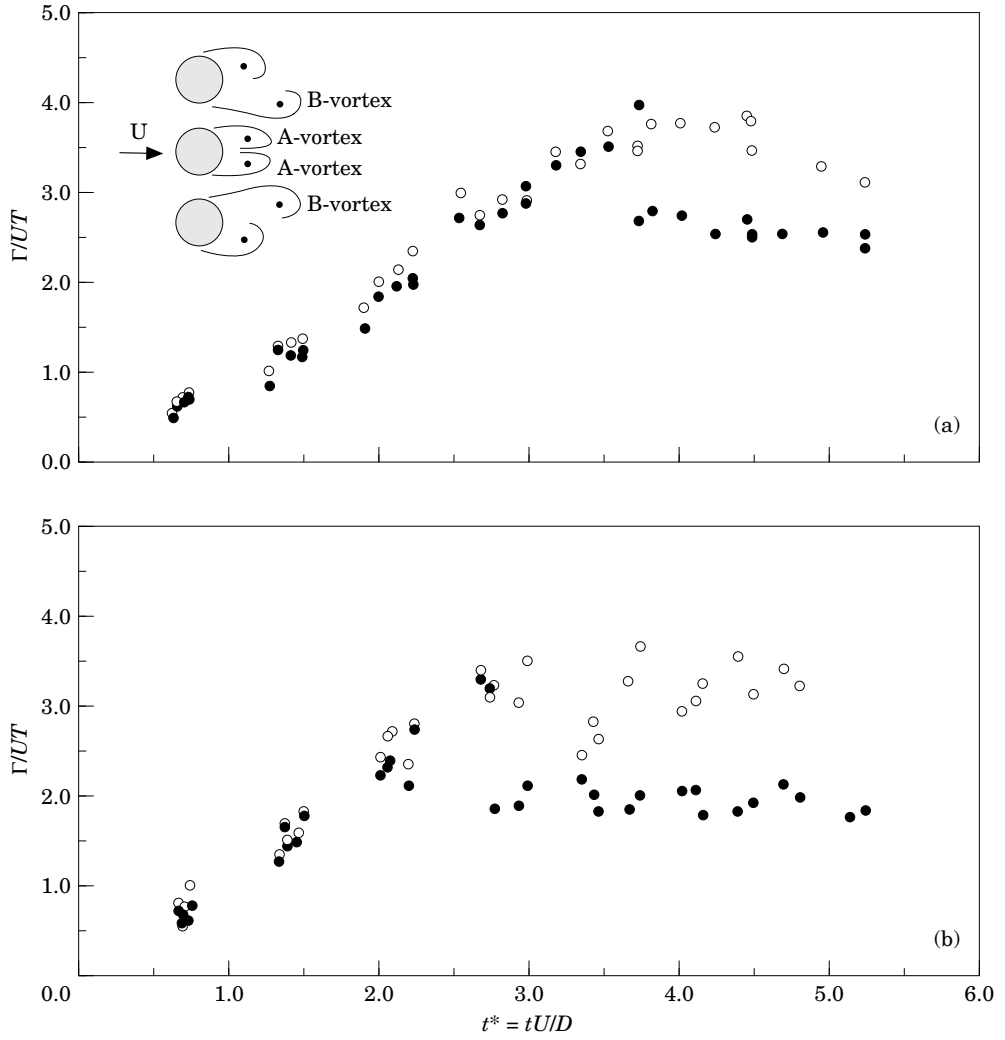

Figure 11. Vortex strength data for three side-by-side circular cylinders with $T/D > 1{\cdot}0$ impulsively set into motion; (○) A-vortices; (●) B-vortices: (a) $T/D = 1{\cdot}5$; (b) $T/D = 2{\cdot}0$.

Circulation data for each of the vortices are shown in Figure 11, and vortex location data a/D and b/D are presented in Figure 12. Asymmetric flow patterns, seen under steady flow conditions (Eastop & Turner 1982; Kumada *et al*. 1984), are not observed under impulsively-started conditions, and it is presumed that any change to such a flow pattern occurs for $t^* > 5{\cdot}0$–$6{\cdot}0$.

7. FURTHER DISCUSSION

Comparison of circulation data for two- and three-cylinder configurations shows that the temporal development of the attached gap vortex strength is similar for both configurations, i.e. it is apparently independent of the number of cylinders. Furthermore, a comparison of the strength of shed gap vortices, comprising the counter-rotating vortex pair in the far wake, is shown in Figure 13 to scale uniquely with the

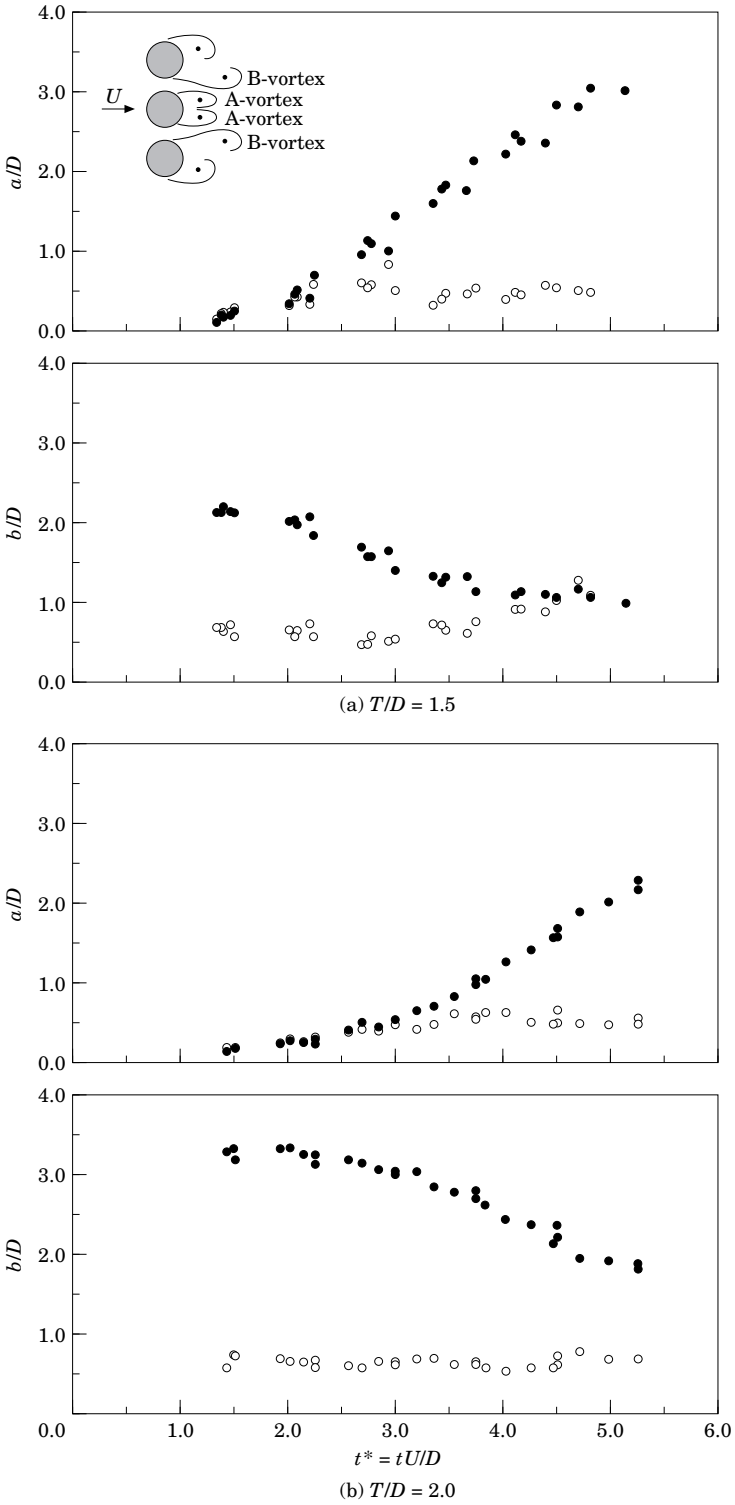

Figure 12. Vortex centre position data a/D and b/D for three side-by-side circular cylinders with $T/D > 1{\cdot}0$ impulsively set into motion; (○) A-vortices; (●) B-vortices: (a) $T/D = 1{\cdot}5$; (b) $T/D = 2{\cdot}0$.

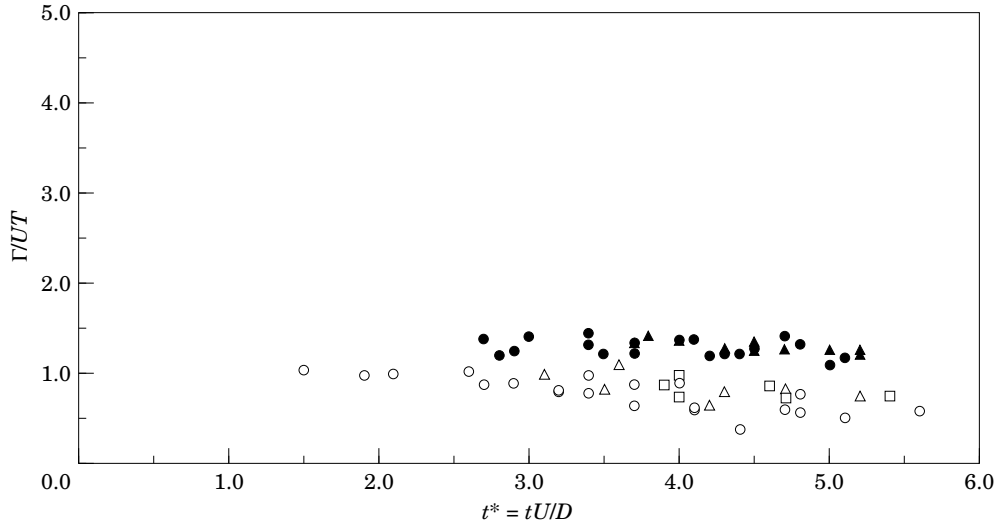

Figure 13. Strength of a vortex comprising the far wake counter-rotating vortex pair for different impulsively-started side-by-side circular cylinder configurations. Two cylinders: (○) $T/D = 1{\cdot}5$; (△) $T/D = 2{\cdot}0$; (□) $T/D = 2{\cdot}5$. Three cylinders: (●) $T/D = 1{\cdot}5$; (▲) $T/D = 2{\cdot}0$.

transverse pitch T rather than the cylinder diameter D. This result indicates that the strength of the counter-rotating vortex pair is proportional to the proximity of the cylinders, and by consequence to the transverse separation b/D of the initially-formed gap vortices. This result is consistent with a counter-rotating vortex pair not being observed for two cylinders at $T/D = 3{\cdot}0$, since interaction and mutual attraction of the gap vortices is weakened.

8. CONCLUSIONS

This study represents a first quantitative investigation of side-by-side circular cylinders under conditions of impulsively-started cross-flow, using particle image velocimetry (PIV). This approach permits the flow patterns to be visualized and quantified through measurements of the in-plane instantaneous vorticity field, the vortex positions, and the vortex strengths. For configurations of $T/D = 1{\cdot}0$ there is a cursory degree of similarity to the single cylinder, for the positions of the vortex centres as well as the nondimensional circulation of these vortices. For configurations with $T/D > 1{\cdot}0$, strong flow through the gap(s) between the cylinders and vortices formed alongside the gap(s) tend to dominate the fluid behaviour. This strong gap flow quickly initiates (i) breakup of the recirculation zones that form behind each of the cylinders and (ii) vortex shedding. Near-wake regions of individual cylinders are asymmetrical and biased towards this gap flow, with the exception of the central cylinder of the three-cylinder configuration, which remains symmetrical. For both the two- and three-cylinder configurations, there is strong interaction between the gap vortices, particularly for small T/D. In many cases, the far-wake region is marked by the formation of a single counter-rotating vortex pair, the strength of which is independent of T/D when T is used to nondimensionalize the circulation.

ACKNOWLEDGMENTS

The authors would like to acknowledge the financial support of the Natural Sciences and Engineering Research Council of Canada (NSERC) and Les Fonds FCAR du

Québec. The assistance of Olivier Lefebvre, who conducted some of the experiments, is also appreciated. The authors would also like to thank J. M. Anderson and M. S. Triantafyllou of the Massachusetts Institute of Technology, in matters concerning the digital PIV technique.

References

Bearman, P. W. & Wadcock, A. J. 1973 The interaction between a pair of circular cylinders normal to a stream. *Journal of Fluid Mechanics* **61,** 499–511.

Bouard, R. & Coutanceau, M. 1980 The early stage of development of the wake behind an impulsively-started cylinder for $40 < \mathrm{Re} < 10^4$. *Journal of Fluid Mechanics* **101,** 583–607.

Chu, C. C. & Liao, Y. Y. 1992 A quantitative study of flow around an impulsively started circular cylinder. *Experiments in Fluids* **13,** 137–146.

Coutanceau, M. & Bouard, R. 1977 Experimental determination of the main features of the viscous flow in the wake of a circular cylinder in uniform translation. Part 2. Unsteady flow. *Journal of Fluid Mechanics* **79,** 257–272.

Eastop, T. D. & Turner, J. R. 1982 Air flow around three cylinders at various pitch-to-diameter ratios for both a longitudinal and transverse arrangement. *Transactions of the Institution of Chemical Engineers* **60,** 359–363.

Honji, H. & Taneda, S. 1969 Unsteady flow past a circular cylinder. *Journal of the Physical Society of Japan* **27,** 1668–1677.

Kumada, M., Hiwada, M., Ito, M. & Mabuchi, I. 1984 Wake interference between three circular cylinders arranged side-by-side normal to a flow. *Transactions of the JSME* **50**(455), 1699–1707 (in Japanese).

Nagata, H., Kakehi, Y., Tsunekawa, M. & Hasegawa, T. 1975 Unsteady flow past a circular cylinder started impulsively. *Bulletin of the JSME* **18**(123), 992–1001.

Nagata, H., Minami, K. & Murata, Y. 1979 Initial flow past an impulsively started circular cylinder. *Bulletin of the JSME* **22**(166), 512–520.

Nagata, H., Funada, H., Kawai, K. & Matsui, T. 1985a Unsteady flows in the vortex region behind a circular cylinder started impulsively (1st report, feeding mechanism of vorticity and onset of turbulence). *Bulletin of the JSME* **28**(245), 2599–2607.

Nagata, H., Funada, H. & Matsui, T. 1985b Unsteady flows in the vortex region behind a circular cylinder started impulsively (2nd report, velocity fields and circulations). *Bulletin of the JSME* **28**(245), 2608–2616.

Nagata, H., Nagase, I. & Ito, K. 1989 Unsteady flows past a circular cylinder started impulsively in the Reynolds number range $500 < \mathrm{Re} < 10\,000$. *JSME International Journal,* Series II **32,** 540–549.

Sarpkaya, T. 1991 Nonimpulsively started steady flow about a circular cylinder. *AIAA Journal* **29,** 1283–1289.

Sumner, D., Price, S. J. & Païdoussis, M. P. 1997a Side-by-side circular cylinders in impulsively-started flow. Submitted to the *16th Canadian Congress of Applied Mechanics,* Québec City, Canada, pp. 271–272.

Sumner, D., Wong, S., Price, S. J. & Païdoussis, M. P. 1997b Two and three side-by-side circular cylinders in steady cross-flow. *Proceedings of the 16th Canadian Congress of Applied Mechanics*, Québec City, Canada, pp. 273–274.

Taneda, S. & Honji, H. 1971 Unsteady flow past a flat plate normal to the direction of motion. *Journal of the Physical Society of Japan* **30,** 262–272.

Ta Phuoc Loc & Bouard, R. 1985 Numerical solution of the early stage of the unsteady viscous flow around a circular cylinder: a comparison with experimental visualization and measurements. *Journal of Fluid Mechanics* **160,** 93–117.

Willert, C. & Gharib, M. 1991 Digital particle image velocimetry. *Experiments in Fluids* **10,** 181–193.

Williamson, C. H. K. 1985 Evolution of a single wake behind a pair of bluff bodies. *Journal of Fluid Mechanics* **159,** 1–18.

Wu, C. L. & Chu, C. C. 1989 The flow around an impulsively started circular cylinder: a preliminary study. *Proceedings of the 13th Annual Conference on Mechanics,* Taiwan, pp. 727–735; cited in Chu & Liao (1992).